ESRF	**Experiment title:** Phase separation and lattice distortions in $Y_{1-x}Pr_xBa_2Cu_3O_y$ compositions	**Experiment number**: CH 2013
Beamline: BM01B	**Date of experiment**: from: 16/02/2006 to: 21/02/2006	**Date of report**: 01/09/2006
Shifts: 9	**Local contact(s)**: H. EMERICH and W. VAN BEEK	*Received at ESRF:*

Names and affiliations of applicants (* indicates experimentalists):

M. Calamiotou*, A. Gantis, University of Athens, GR 157 84, Athens, Greece

E. Liarokapis*, D. Palles*, Technical University of Athens, GR 157 80, Athens, Greece

I.Mariolaki*, ESRF, BP 220,38043 Grenoble Cedex, France

Report:

We have measured fully refinable high resolution diffraction patterns at **15K** for **8** compositions of the superconductive oxide $\mathbf{Y_{1-x}Pr_xBa_2Cu_3O_y}$ **(0.0≤x≤1.0),** which have been synthesised in our laboratory**.** The $Y_{1-x}Pr_xBa_2Cu_3O_y$ **(YPr123)** compound is the most puzzling one among all other superconducting cuprates, the mechanism, which suppresses superconductivity when Pr substitutes for Y, remaining still obscure. Different mechanisms such as hole filling, pair breaking, hybridisation as well as Pr partial substitution for Ba have not found complete justification from the different experimental results. In addition the role of Pr induced structural and electronic *inhomogeneities*, which manifest themselves by the formation of three subphases, as evidenced from our Raman spectroscopy results, needs further examination. Such phase separation effects are expected to correlate with microstructural characteristics and lattice distortions. The purpose of our experiments was to systematically investigate the subtle structural and microstructural changes in the solid solution by using Synchrotron High Resolution Powder Diffraction data in combination with Raman spectroscopy results. We have investigated the correlation of any microstrustural as well as any local structural changes induced by Pr doping in Y123 with spectral modifications of the Raman-active phonons and the reduction in T_c. The role of Pr substitution for Ba was also investigated based on the results obtained by both methods.

In our initial proposal for beamline **ID31**, we planed to measure fully refinable diffraction patterns at both 5K and RT for the 16 compositions available. Due to the different characteristics of beamline **BM01**, where we have performed the experiments, it was possible to measure during the available time only 8 compositions, covering the doping range x=0.0-1.0, only at one temperature (T=15K).

The XRD patterns (collected at λ=0.60008Å with a 0.7mm-diameter quarzt capillary for a 2θ range 0.5-45.5^o) were refined using the GSAS suite of Rietveld analysis programms in the orthorhombic space group Pmmm (Fig.1). The diffraction lines were modeled by a pseudo-Voigt function with axial divergence aymmetry corrections and the microstrain broadening description of P. Stephens (J. Appl. Cryst.,**32**,281 (1999) (CW profile function 4 in GSAS). The secondary phase $BaCuO_2$ indicative of the presence of Pr/Ba antisite defects was included in the refinement. The isotropic thermal factors for all atoms and the Pr/Ba antisite defects have been also separetly refined. Based on the up to now analysis of our XRD data, the following new results have been obtained: *Microstructural characteristics* ---- Anisotropic broadening of Bragg peaks, the 00*l* reflections beeing sharper than the *hkl* ones (Fig.2), is evident in the XRD patterns for the whole composition range. This indicates that lattice distortions are predominent in the basal a-b plane. Microstrains along the c-axis, calculated from the refined Stephens coeffisients, are two orders of magnitude smaller than the

corresponding along the a and b axis, in consinstance with the high anisotropy of the Y123 material. Microstrains seem to increase with Pr doping. However, for compositions $0.3 \leq x \leq 0.8$ microstrains remain almost constant (Fig.3a, dashed lines are guide to the eye). For the same compositional range the size of the presumably spherical coherently diffractiong domains estimated from the Lorenztian contribution to broadening L_x according to $P(\mu m)=(180/\pi)\cdot(0.9\lambda/L_x 100)$ show minimum values (Fig.3b). The origin of anisotropic peak broadening is still a subject of further investigations. The evolution of the microstructural features with Pr doping correlates with the observed by Raman spectroscopy development of three bands, attributed to three subphases (Fig.4), allthough no direct evidence has been found up to now by the XRD results of phase separation effects. *Structural characteristics* --- The a and b lattice parameters are linearly increasing (the orthorhombic strain remaining allmost constant in the whole compositional range) with nominal Pr content x, in accordance with the bigger Pr replacing the smaller Y ion. On the contrary, the c lattice parameter does not show a significant change. A systematic increase of the in-plain Cu_{pl}-O_{pl} bonds and the Pr-O_{pl} bonds is observed following the increase of the a,b, lattice constants. Pr/Ba antisite defects are systematically increasing (up to 13% per Ba atom) upon Pr doping (Fig.5). An increase of the isotropic atomic displacement factor at the Ba site upon Pr doping has been also observed.

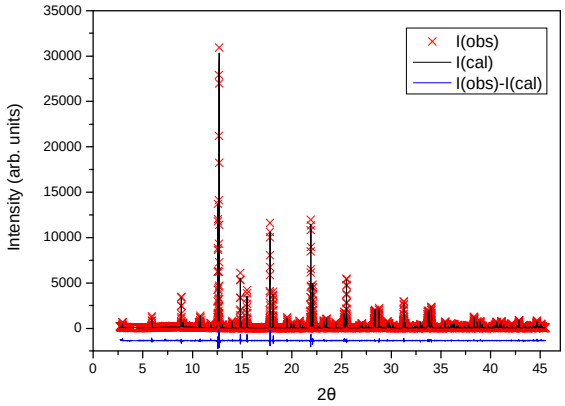

Fig.1 Example of Rietveld fit of orthorhombic (*Pmmm*) Y123 at 15K (BM01, λ=0.60008Å) χ^2=2.79, R_{wp}=12.21%, R_F^2 =3.23%

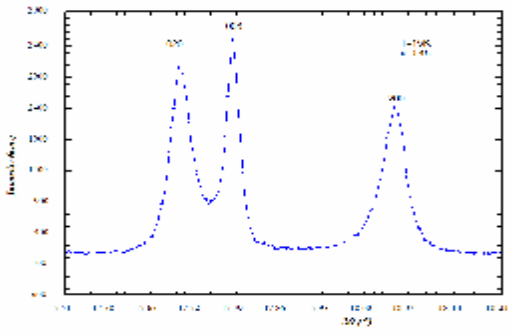

Fig. 2: 020, 006 and 020 reflections for $Y_{0.55}Pr_{0.45}Ba_2Cu_3O_y$ at 15K

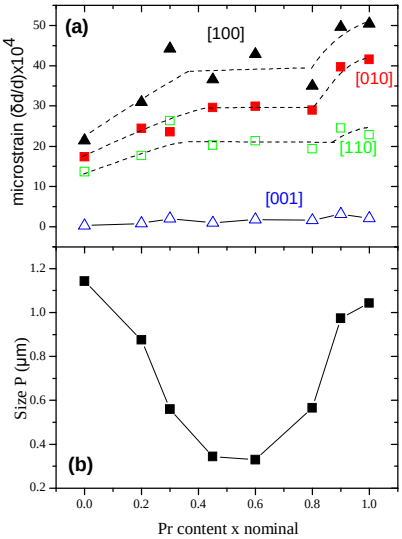

Fig 3: Variation of **(a)** microstrain (δd/d) along different directions **(b)** size P of coherently diffracting domains vs. the Pr nominal content (Lines are guide to the eye).

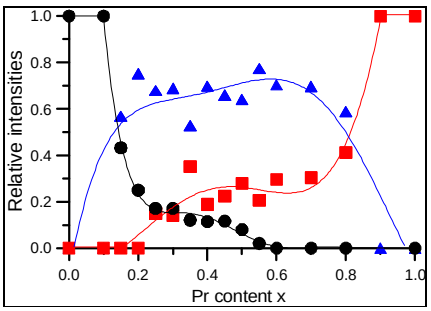

Fig.4 : Variation of amount of subphases vs. the Pr nominal content (• $Y_{1-x}Pr_x123$ phase, ■ $Y_{1-x}Pr_x123$, ▲ $Y_{1-x}Pr_x123$). Lines are guide to the eye.

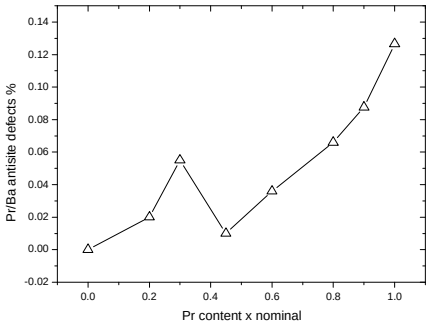

Fig.5: Variation Pr/Ba antisite defects vs. Pr nominal content (x).